Behavior and design of slender FRP-confined circular RC columns

T. Jiang[1] and J.G. Teng[2,*]
[1]Zhejiang Provincial Key Laboratory of Space Structures
Department of Civil Engineering
Zhejiang University, Hangzhou, Zhejiang Province, China
[2]Department of Civil and Structural Engineering
The Hong Kong Polytechnic University, Hong Kong, China
*cejgteng@polyu.edu.hk

Abstract: Strengthening of reinforced concrete (RC) columns through lateral confinement using fiber-reinforced polymer (FRP) jackets is now a widely accepted technique. While extensive research has been conducted on the behavior of such strengthened columns, only a very limited amount of work has examined the slenderness effect in these columns. To correct this deficiency, the present paper presents a systematic study on the subject and proposes the first ever design method for slender FRP-confined circular RC columns. A simple theoretical column model for such columns is first described in the paper. Numerical results obtained from this theoretical model are then presented to examine the behavior of these columns to identify the key parameters of influence. A design method based on numerical results from the column model and following the nominal curvature approach is next formulated. The accuracy and safety of the proposed design method is demonstrated through comparison with existing experimental results.

Key words: FRP; concrete; confinement; slender columns; design

1 Introduction

Strengthening of reinforced concrete (RC) columns using fiber-reinforced polymer (FRP) jackets (or wraps) is now a widely accepted technique. This technique is particularly effective for circular columns as the strength and ductility of concrete in a circular section can be substantially increased through lateral confinement with FRP. Although less effective, FRP jacketing has also been widely used in the strengthening of rectangular RC columns. All discussions in this paper are limited to circular RC columns.

To facilitate the practical application of the technique to circular RC columns, relevant design provisions have been developed through extensive research (e.g. Teng et al. 2002) and are now included in various design guidelines for the FRP strengthening of RC structures (fib 2001; ISIS 2001; ACI-440.2R 2002, 2008; CNR-DT200 2004; Concrete Society 2004). All these design provisions, however, suffer from one important limitation: the effect of column slenderness (i.e. the second-order effect) is not included; that is, all these design provisions are limited to the design of FRP jackets for short columns for which the second-order effect is negligible. This limitation can be attributed to the limited amount of research on the behavior of slender FRP-confined RC columns. On the experimental side, Tao et al. (2004),

Fitzwilliam and Bisby (2010) and Bisby and Ranger 2010) tested FRP-confined RC columns with a height-to-diameter ratio up to 20.4. Tamuzs et al. (2007a) also tested FRP-confined RC columns with a height-to-diameter ratio of 4, but little slenderness effect existed in these columns as a result of their relatively small slenderness and end conditions. In addition, De Lorenzis et al. (2004) and Tamuzs et al. (2007b, 2008a) tested slender FRP-confined concrete columns without steel reinforcement subjected to concentric compression to investigate the stability of these columns. On the theoretical side, Tamuzs et al. (2008b) proposed an analytical solution for the prediction of the buckling load of FRP-confined RC columns subjected to concentric compression. Jiang and Teng (2012a) developed a theoretical column model capable of modeling the behavior of slender FRP-confined RC columns. The limited existing research has nevertheless allowed the following two important observations to be made: (a) an RC column which is originally classified as a short column may need to be treated as a slender column after FRP jacketing; and (b) the effectiveness of FRP confinement in enhancing the load-carrying capacity of an RC column decreases as the column becomes more slender. These phenomena are both due to the fact that FRP confinement can substantially increase the axial load capacity of an RC section, but its flexural rigidity in the range of confinement-enhanced resistance is much lower than the initial flexural rigidity.

The above discussions suggest that there is a real need to develop a rational design procedure for slender FRP-confined RC columns. Indeed, the first of the two observations mentioned above means that the effect of column slenderness is a more wide-spread problem for FRP-confined RC columns than for their unconfined counterparts. Against this background, a series of systematic studies on slender FRP-confined circular RC columns has recently been conducted by the present authors. Jiang and Teng (2012a) developed a rigorous theoretical model for slender FRP-confined circular RC columns. This theoretical model was then employed by Jiang and Teng (2012b) to generate numerical results for the formulation of a slenderness limit for the differentiation of slender columns from short columns. This paper presents a follow-on study which was undertaken to develop a design procedure for slender FRP-confined circular RC columns.

In practice, the majority of columns are restrained at both ends and are eccentrically loaded, with the two end eccentricities being generally different. However, such a restrained column with different end eccentricities can be transformed into an equivalent hinged column with equal end eccentricities using the well-known effective length approach (Kavanagh 1960; Jiang 2008); this equivalent column is referred to as the standard hinged column herein. This paper is therefore limited to the behavior and design of slender FRP-confined circular RC columns which are standard hinged columns.

The paper first describes a simple theoretical slender column model for standard hinged RC columns confined with FRP. This is followed by the presentation of a parametric study which was performed to determine the maximum allowable amount of FRP confinement and the slenderness limit of RC columns beyond which the use of FRP for strengthening may become uneconomical and is thus not recommended. Finally, a design method based on numerical results from the column model and following the nominal curvature approach is proposed, and its accuracy and safety is demonstrated through comparison with existing experimental results.

The present study was partially motivated by the need to formulate design provisions for the Chinese national standard entitled "Technical Code for Infrastructure Application of FRP Composites" (GB-50608 2010), which has come into force in 2011. This new standard has been developed within the framework of the current Chinese code for the design of concrete structures (GB-50010 2002). Therefore, some of the considerations in this paper follow the specifications given in GB-50010 (2002), and these considerations are highlighted where appropriate. These considerations, however, do not distract from the generality of the study.

2 Theoretical model for standard hinged columns

2.1 Assumptions

In the present theoretical column model, the deflected shape of the column is assumed to be a half-sine wave and equilibrium is checked at the maximum-deflection section at column mid-height (i.e. the critical section). This method of analysis has been widely adopted in similar studies of standard hinged columns (e.g. Bazant et al. 1991) and has proven to be very successful. Besides the above fundamental assumption, the following assumptions were also adopted in developing this theoretical column model: (a) the lateral deflection of the column is small in comparison with its length; (b) plane sections remain plane; (c) the steel reinforcement has an elastic-perfectly plastic stress-strain curve; (d) any confinement from transverse steel reinforcement is negligible; (e) the concrete does not resist any tension; and (f) the stress-strain behavior of FRP-confined concrete in compression can be represented by Lam and Teng's stress-strain model as detailed in the subsequent sub-section; (g) the stress-strain curves of steel and FRP-confined concrete are both reversible during unloading (i.e. the two materials are assumed to be nonlinear elastic materials). Assumption (d) means that the present work is inapplicable to RC columns which receive significant confinement from lateral steel reinforcement. Assumption (f) assumes that the stress-strain behavior of FRP-confined concrete in an eccentrically-loaded column is the same as that of FRP-confined concrete under concentric compression. Jiang and Teng (2012a) have shown that this assumption leads to reasonably accurate predictions for the axial load capacity of eccentrically-loaded FRP-confined RC columns although the possible effect of eccentricity on the effectiveness of FRP confinement needs to be further clarified (Jiang and Teng 2012a). The final assumption simplifies the analysis and affects little the predictions of the theoretical model as has been shown by Bazant et al. (1991).

2.2 Lam and Teng's stress-strain model for FRP-confined concrete

Lam and Teng's stress-strain model was originally presented in Lam and Teng (2003). The original Lam and Teng model has been adopted by both UK's Concrete Society (2004) design guideline and the ACI-440.2R (2008) guideline for strengthening concrete structures. Lam and Teng's model adopts a simple form (a parabolic first portion which connects smoothly to a linear second portion) which automatically reduces to that for unconfined concrete when no FRP is provided (see Fig. 1). This simple form is described by the following expressions:

$$\sigma_c = E_c\varepsilon_c - \frac{\left(E_c - E_2\right)^2}{4f_{co}^{'}}\varepsilon_c^2 \quad \text{for} \quad 0 \le \varepsilon_c < \varepsilon_t \tag{1a}$$

$$\sigma_c = f_{co}^{'} + E_2\varepsilon_c \quad \text{for} \quad \varepsilon_t \le \varepsilon_c \le \varepsilon_{cu} \tag{1b}$$

where σ_c and ε_c are the axial stress and the axial strain respectively, E_c is the elastic modulus of unconfined concrete, E_2 is the slope of the linear second portion, and $f_{co}^{'}$ is the compressive strength of unconfined concrete. The transition strain ε_t between the parabolic first portion and the linear second portion and the slope of the linear second portion E_2 are respectively given by:

$$\varepsilon_t = \frac{2f_{co}^{'}}{E_c - E_2} \tag{2}$$

$$E_2 = \frac{f_{cc}^{'} - f_{co}^{'}}{\varepsilon_{cu}} \tag{3}$$

where $f_{cc}^{'}$ and ε_{cu} are respectively the compressive strength and the ultimate axial strain of confined concrete. The expressions for $f_{cc}^{'}$ and ε_{cu} have been recently refined by Teng et al. (2009) based on recent test results and an accurate analysis-oriented stress-strain model for FRP-confined concrete (Teng et al. 2007; Jiang and Teng 2007). These new expressions are given by:

$$\frac{f_{cc}^{'}}{f_{co}^{'}} = \begin{cases} 1 & \text{if } \rho_K < 0.01 \\ 1 + 3.5\left(\rho_K - 0.01\right)\rho_\varepsilon & \text{if } \rho_K \ge 0.01 \end{cases} \tag{4}$$

$$\frac{\varepsilon_{cu}}{\varepsilon_{co}} = 1.75 + 6.5\rho_K^{0.8}\rho_\varepsilon^{1.45} \tag{5}$$

where $\rho_K = 2E_{frp}t/(E_{\text{sec}o}D)$ is the confinement stiffness ratio, $\rho_\varepsilon = \varepsilon_{h,rup}/\varepsilon_{co}$ is the strain ratio, D is the diameter of the confined column, E_{frp} is the elastic modulus of FRP in the hoop direction, t is the thickness of the FRP jacket, $\varepsilon_{h,rup}$ is the hoop rupture strain of the FRP jacket, and $E_{\text{sec}o}$ and ε_{co} are the secant modulus and the axial strain at the compressive strength of unconfined concrete, with $E_{\text{sec}o} = f_{co}^{'}/\varepsilon_{co}$. When this model is used in a design specification, the model may need small adjustments so that the curve reduces to that for unconfined concrete in a specific

national code. In GB-50010 (2002), normal strength concrete is assumed to have $\varepsilon_{co} = 0.002$ and an ultimate axial strain of 0.0033. As a result, $E_c = 1000 f_{co}^{'}$ and the original value of 1.75 for the first term on the right hand side of Eq. 5 is replaced by 1.65 in the present study, so that the stress-strain model for FRP-confined concrete reduces to that for unconfined normal strength concrete adopted by GB-50010 (2002) when no FRP is provided. It should be noted that the refined version of Lam and Teng's stress-strain model with the above two adjustments was used in all the calculations reported in the present paper. For brevity, this refined version of Lam and Teng's model as employed in the present theoretical column model is referred to simply as Lam and Teng's model hereafter in this paper.

2.3 Method of analysis

The assumption that the deflected shape of the standard hinged column can be closely approximated using a half-sine wave can be mathematically expressed as:

$$f = -f_{mid} \sin\left(\frac{\pi}{l} x\right) \tag{6}$$

where f_{mid} is the lateral displacement (more precisely the magnitude of the lateral displacement) at the column mid-height (i.e. the critical section), x is the distance along the column axis from the origin (i.e. the bottom support), and l is the length of the standard hinged column (Fig. 2). Differentiating Eq. 6 twice gives:

$$\phi = f_{mid} \frac{\pi^2}{l^2} \sin\left(\frac{\pi}{l} x\right) \tag{7}$$

where ϕ is the curvature of the column at the height of x. Therefore, f_{mid} is related to the curvature at the column mid-height ϕ_{mid} through:

$$f_{mid} = \frac{l^2}{\pi^2} \phi_{mid} \tag{8}$$

The moment acting on the mid-height section can then be written as:

$$M_{mid} = N\left(e + f_{mid}\right) = N\left(e + \frac{l^2}{\pi^2} \phi_{mid}\right) \tag{9}$$

where N is the axial load, e is the load eccentricity at column ends. This moment must be resisted by the stresses on the mid-height section. These stresses can be determined from a conventional section analysis in which numerical integration over the section is carried out using the layer method and Lam and Teng's stress-strain model is assumed for the confined concrete. Details of such a section analysis can be

found in Jiang and Teng (2012a) and is thus not given here due to space limitation. In the present column model, it is more convenient to seek the values of M_{mid} and N for a given value of f_{mid}. That is, for a given value of f_{mid}, evaluate the corresponding value of ϕ_{mid} using Eq. 8; a strain value for the extreme compression fiber of concrete can then be assumed to evaluate the resultant axial force and moment of the mid-height section to see if their values satisfy the relationship defined by Eq. 9. Once Eq. 9 is satisfied, the solution for the present value of f_{mid} is found. Otherwise, the assumed strain value should be adjusted until Eq. 9 is satisfied. Once the solution for the present value of f_{mid} is found, a point on the full-range load-deformation curve of the column is identified; the entire curve can be generated by finding successive values of M_{mid} and N for increasing values of f_{mid}. The analysis stops when the extreme compression fiber of concrete reaches its ultimate axial strain as defined by Lam and Teng' stress-strain model. In the present study, the mid-height section was divided into 50 horizontal layers and the solution was considered converged when the difference between the two sides of Eq. 9 is within $10^{-6}M_{mid}$. A computer program was written using Matlab 7.1 to implement the above numerical procedure.

It should be noted that the authors also developed a more rigorous theoretical column model for which no assumption needs to be made about the deflected shape of the column (Jiang and Teng 2012a). That column model was used in the development of a slenderness limit to define short FRP-confined circular RC columns (Jiang and Teng 2012b). This slenderness limit allows short columns to be identified at the initial stage of design so that the additional complexity involved in the design of slender columns can be avoided. An important feature of Jiang and Teng's (2012a) column model is its ability to deal with unequal column end eccentricities. This feature allows the effect of the end eccentricity ratio (i.e. the ratio between the two end eccentricities) on the slenderness limit to be studied. The simple column model was employed in the present study as for standard hinged columns as it requires much less computational effort but leads to predictions which are only about 1% to 2% higher than the predictions of the more rigorous model (Jiang 2008). Indeed, the approach of the simple column model forms the analytical basis of design equations for slender RC columns specified in existing design codes (e.g. ENV-1992-1-1 1992; GB-50010 2002).

3 Limits on the use of FRP

In the design of FRP jackets for the strengthening of RC columns, it is important to ensure that the FRP material is used in a safe and economical manner. Existing tests on small-scale FRP-confined circular concrete cylinders have shown that the concrete strength can be greatly increased (e.g. more than tripled) provided the FRP confinement is strong enough (e.g. Jiang and Teng 2007). The failure of strongly-confined circular concrete specimens can, however, be explosive and is undesirable in practice. Existing studies have also shown that the effectiveness of FRP confinement reduces as columns become more slender (e.g. Tao et al. 2004; Fitzwilliam and Bisby 2010; Jiang and Teng 2012a), thus the use of FRP becomes uneconomical for very slender columns. Another design concern with FRP-confined RC columns is that the lateral deflection may exceed an acceptable limit. It is thus advisable to impose certain limits on the use of FRP to ensure that the FRP is used in a safe and

economical manner. To this end, a parametric study was conducted using the simple theoretical column model presented in the preceding section to examine how the effectiveness of FRP confinement is affected by various parameters (Jiang 2008).

The parametric study was carried out on a reference circular RC column, as shown in Fig. 2. The reference column had a diameter of 600 mm and was longitudinally reinforced with 12 evenly distributed steel bars. These two geometric properties were also used in obtaining numerical results for demonstration cases throughout the paper (Figs 5-7 and Fig. 9). The diameter of the circle defined by the centers of steel bars is denoted by d. The strengths of concrete and steel reinforcement were taken to be common values as specified in GB-50010 (2002). The concrete was assumed to be grade C30, representing a characteristic cube strength $f_{cu}^{'} = 30$ MPa and a corresponding cylinder strength $f_{co}^{'} = 0.67 f_{cu}^{'} = 20.1$MPa. The steel was assumed to be grade II with a characteristic yield strength $f_y = 335$ MPa and an elastic modulus $E_s = 200$ GPa. Fixed values of $f_{co}^{'}$ and f_y were used in the parametric study and other numerical demonstration cases throughout the paper because previous studies (Pfrang and Siess 1961; MacGregor et al. 1970) have shown that these two parameters affect only slightly the effect of slenderness. The variable parameters considered include the slenderness ratio λ (i.e. the ratio of the effective length of a column to the radius of gyration of the column section), the normalized eccentricity e/D, the longitudinal steel reinforcement ratio ρ_s, the depth ratio d/D, the strength enhancement ratio $f_{cc}^{'}/f_{co}^{'}$ and the strain ratio ρ_ε. The last two parameters represent the effect of FRP confinement. As specified in GB-50010 (2002), $\varepsilon_{co} = 0.002$ was adopted in the parametric study. The values used for these parameters are summarized in Table 1. The combinations of these parameters led to about 8,000 cases. The slenderness ratio went up to 50 as a preliminary study showed that beyond this slenderness the strengthening effect of FRP is very limited. The values used for the remaining parameters are the same as those reported in Jiang and Teng (2012b) where detailed justifications for the values used can be found.

The numerical results of the parametric study confirmed that: 1) strong confinement may result in excessive column lateral deflection that is not acceptable in design; and 2) the effectiveness of FRP confinement in enhancing the column strength reduces rapidly as the column slenderness increases. Therefore, the following two limits were proposed based on the numerical results from the parametric study (Jiang 2008) to ensure a safe and economical strengthening design:

$$\frac{f_{cc}^{'}}{f_{co}^{'}} \le 1.75 \tag{10}$$

$$\lambda_{\max} = 50 - 3\rho_\varepsilon \tag{11}$$

The numerical results indicated (Jiang 2008) that with the above two limits: 1) a 10% increase in the column axial load capacity can be realized in most cases while the maximum possible increase is approximately 50%; and 2) the column lateral

deflection at failure is within the commonly accepted limit of $l/50$ in design (Cranston 1972). A full presentation and discussion of the parametric study can be found in Jiang (2008).

Some of the values listed in Table 1 do not satisfy the conditions set by Eqs 10 and 11; these values were thus removed to form a reduced set of parameters for use in the formulation of the design method. The values of the parameters in the reduced set are listed in Table 2. It should be noted that the values of $\lambda_{\max}$ defined by Eq. 11 for the three different strain ratios considered are 47, 38.75, and 27.5 respectively. Values of 50, 40, and 30 were however used instead for simplicity.

4 Design method

4.1 Review of current design methods for RC columns

The current design approach included in various design codes for RC columns (e.g. ENV-1992-1-1 1992; BS-8110 1997; GB-50010 2002; ACI-318 2008) approximates the second-order moment by an amplification of the first-order moment so that the failure load can be related to the strength of the critical section. In other words, the current design approach transforms the design of a slender column into the design of a section with an equivalent eccentricity, which consists of the initial end eccentricity of the slender column and a an additional eccentricity equal to the nominal lateral displacement of the critical section f_{nom}. The concept of this additional eccentricity is illustrated in Fig. 3. Fig. 3 shows three possible loading paths as solid lines (OA, OB and ODE) for a standard hinged column with three different values of column slenderness but a fixed initial end eccentricity. Loading path OA is for zero slenderness in which case the slenderness effect is absent; loading path OB is for an intermediate slenderness in which case the column is controlled by material failure; loading path ODE is for a large slenderness in which case the column is controlled by stability failure. Graphically, the design approach seeks the straight loading paths OB and OC (shown as dashed lines) to replace the original curved loading paths OB and ODE (shown as solid lines) for material failure and stability failure respectively. It is obvious that for material failure, f_{nom} is the real lateral displacement of the critical section at failure. However, for stability failure, f_{nom} is a fictitious lateral displacement. This point must be borne in mind and is further discussed later. It is now clear that the key element of the current design approach is to find f_{nom}.

There are two main methods in the current design codes for the evaluation of the amplified moment, namely, the moment magnifier method and the nominal curvature method. The moment magnifier method has been adopted by ACI-318 (2008) and many of its previous versions, among others. This approach originated from the elastic analysis of columns, where the lateral deflection can be exactly determined provided the section flexural stiffness is known. When this approach is used for the design of RC columns, the key is to find the equivalent section flexural stiffness that accounts for the effect of material nonlinearity. By contrast, the nominal curvature method was originally proposed by Aas-Jakobsen and Aas-Jakobsen (1968) and has been adopted by ENV-1992-1-1 (1992), BS-8110 (1997), and GB-50010 (2002), among others. This approach relates the lateral deflection to the curvature through the

relationship defined by Eq. 8. It is obvious that the key to this approach is to determine the nominal curvature ϕ_{nom} corresponding to f_{nom}. This paper follows the nominal curvature approach to develop a design procedure that is consistent with GB-50010 (2002). Therefore, the moment magnifier method is not further discussed in the paper.

4.2 Nominal curvature

According to Eq. 8, the nominal curvature and the nominal lateral displacement can be related by the following equation:

$$f_{nom} = \frac{l^2}{\pi^2}\phi_{nom} \tag{12}$$

As explained earlier, the nominal curvature sought in the nominal curvature method for material failure is the real curvature of the critical section at failure ϕ_{fail}. However, the nominal curvature for stability failure needs some further explanation, which can be achieved by referring to the moment-curvature diagram shown in Fig. 4. Fig. 4 shows the moment-curvature curve of the critical section when the column reaches its axial load capacity N_u. This curve shows how the internal moment varies with the curvature of the critical section under this particular axial load. The curvature at the end of this curve, $\phi_{\sec}$, is the maximum curvature that the critical section can sustain under this particular axial load. The inclined straight line represents how the external moment varies as the curvature at the critical section increases. This inclined line can be mathematically described by Eq. 9: it has a slope of $N_u l^2/\pi^2$ and intersects the vertical axis at a value of $N_u e$. At the point where the inclined line meets the moment-curvature curve, the external moment is equilibrated by the internal moment. It is obvious that for material failure (Fig. 4a), the inclined line must intersect the moment-curvature curve at its end (i.e. $\phi_{nom} = \phi_{fail} = \phi_{\sec}$). However, when stability failure occurs, the above three curvatures have different values, as illustrated in Fig. 4b. When stability failure occurs, the inclined line must meet the moment-curvature curve at the point of failure for moment equilibrium. Therefore, the inclined line must be a tangential to the moment-curvature curve at the point of failure, where the curvature is ϕ_{fail}. The nominal curvature is the curvature at the intersection point between the inclined line and the horizontal line as with this nominal curvature, the moment predicted by Eq. 9 is equal to the section moment capacity at material failure under an axial load equal to N_u. Obviously, the nominal curvature always has a value larger than ϕ_{fail} but smaller than $\phi_{\sec}$.

The failure modes of an RC section can be classified into three categories: 1) balanced failure; 2) compression failure; and 3) tension failure. At balanced failure, the extreme compression fiber of concrete reaches the ultimate compressive strain of concrete when the most highly-tensioned longitudinal steel bar(s) on the opposite side of the section reaches the tensile yield strain. The axial load resisted by the section at balanced failure is denoted by N_{bal}. When compression failure occurs, the concrete

reaches its ultimate compressive strain before the steel reinforcement yields. The axial load at compression failure is always larger than N_{bal}. In a tension failure mode, yielding of steel reinforcement occurs first but the ultimate state is only reached after additional deformation when the extreme compression fiber of concrete reaches the ultimate compressive strain of concrete. The axial load at tension failure is always smaller than N_{bal}. According to the definitions given above, the curvature at balanced failure can be easily found to be:

$$\phi_{bal} = 2\frac{\varepsilon_{cu} + \varepsilon_y}{D + d} \tag{13}$$

where ε_{cu} and ε_y are respectively the ultimate axial strain of FRP-confined concrete and the yield strain of the longitudinal steel reinforcement. ϕ_{bal} is used as the basis to evaluate ϕ_{nom} in the nominal curvature method. For material failure, a factor denoted by ξ_1 is used to reflect the effect of axial load when the axial load is other than N_{bal}. For stability failure, an additional factor denoted by ξ_2 needs to be introduced to account for the difference between ϕ_{nom} and $\phi_{\sec}$. In summary, ϕ_{nom} can be related to ϕ_{bal} using the following equation:

$$\phi_{nom} = \xi_1 \xi_2 \phi_{bal} \tag{14}$$

It can be concluded from the above discussions that N_{bal}, ξ_1 and ξ_2 are the essential elements in the nominal curvature method and they are discussed in detail in the following sub-sections.

4.3 Axial load at balanced failure

GB-50010 (2002) specifies the following equation as an estimate of the axial load at balanced failure for an RC section:

$$N_{bal} = 0.5 f_{co}^{'} A \tag{15}$$

where A is the area of the section. As expected, Eq. 15 is unsuitable for FRP-confined RC sections (Fig. 5). Fig. 5 shows a series of interaction curves for an RC section ($\rho_s = 0.1,\ d/D = 0.8$) without FRP confinement and with different levels of FRP confinement (the FRP jacket was assumed to have $\varepsilon_{h,rup} / \varepsilon_{co} = 3.75$) respectively as predicted by the conventional section analysis. These interaction curves are normalized with respect to the axial load capacity N_{uo} (concentric compression) and moment capacity M_{uo} (pure bending) of the reference RC section when no FRP confinement is provided. The location of balanced failure on each curve is indicated by a distinct marker. It is interesting to note that this location lies considerably above the maximum moment point on the interaction curve when a significant level of FRP

confinement is provided; it also appears that this location moves farther away from the maximum moment point as the confinement level increases. The same observation has also been reported by Cheng et al. (2002). The axial load at balanced failure of an FRP-confined RC section depends on the following four parameters: ρ_s, d/D, $f_{cc}^{'}/f_{co}^{'}$ and $\varepsilon_{h,rup}/\varepsilon_{co}$. To develop an approximate expression for N_{bal}, a simple parametric study was conducted for the reduced set of parameters given in Table 2 using the conventional section analysis. Based on the numerical results, the following simple equation is proposed for FRP-confined RC sections:

$$N_{bal} = 0.8 f_{cc}^{'} A \tag{16}$$

Fig. 6 compares the predictions of Eq. 16 with the numerical results for FRP-confined RC sections from the conventional section analysis. It can be seen that Eq. 16 only provides a rough estimation, but it is shown later that it is sufficiently accurate for design use. The predictions of Eq. 15 for RC sections without FRP confinement are also compared with results from the conventional section analysis in Fig. 6.

4.4 Factors ξ_1 and ξ_2

GB-50010 (2002) specifies the following equation for ξ_1:

$$\xi_1 = \frac{N_{bal}}{N_u} \le 1 \tag{17}$$

while BS-8110 (1997) and ENV-1992-1-1 (1992) employ the equation below:

$$\xi_1 = \frac{N_{uo} - N_u}{N_{uo} - N_{bal}} \le 1 \tag{18}$$

Fig. 7 compares the predictions of Eqs 17 and 18 with results from the conventional section analysis. Fig. 7a is for an RC section while Fig. 7b is for an FRP-confined RC section with $f_{cc}^{'}/f_{co}^{'} = 1.5$. It should be noted that the exact value of N_{bal} was used in comparison to eliminate discrepancies due to the different approximate equations in the above-mentioned design codes. The axial loads and curvatures in Fig. 7 are normalized with respect to N_{bal} and ϕ_{bal} respectively. The small circle in Fig. 7 represents balanced failure while the small square represents the case where the section is subjected to the minimum eccentricity $e_{\min}$ as specified in existing design codes for RC structures [e.g. $e_{\min} = 0.05D \le 20\text{mm}$ in BS-8110 (1997) and $e_{\min} = 0.1D$ in ACI-318 (2008)]. The definition for the minimum eccentricity in BS-8110 (1997) was adopted in the present study. It can be seen that the curvature decreases as the axial load increases, and in the case of concentric compression the curvature becomes zero. Although Eq. 18 satisfies the boundary condition at

concentric compression, the overall performance of Eq. 17 is better; this is particularly so as the small range beyond the small square is excluded by the minimum eccentricity and thus does not need to be considered in design. When FRP confinement is provided, the range corresponding to compression failure (i.e. beyond the balanced failure point in Fig. 7b) becomes smaller. It is interesting to note that although the exact results indicate that the curvature at tension failure is always larger than ϕ_{bal}, it is limited to ϕ_{bal} in all the codes mentioned above. This limit on ξ_1 is not explained in Aas-Jakobsen and Aas-Jakobsen (1968) in which the nominal curvature method was originally proposed. To the best of the authors' knowledge, this issue has not been clearly explained so far. An attempt is made below to explain this issue.

When assessing the role played by ξ_1 in the nominal curvature method, it is advisable to combine ξ_1 with ξ_2 to see the overall effect of these two factors. GB-50010 (2002) specifies the following equation for ξ_2:

$$\xi_2 = 1.15 - 0.01\frac{l}{D} \le 1 \tag{19}$$

ξ_2 is limited to 1 because when a column is relatively short it fails in the mode of material failure. It has already been explained that for material failure, only ξ_1 needs to be considered and ξ_2 is always equal to 1 (Fig. 4a). Only when the column is slender enough to suffer stability failure does ξ_2 need to be considered. In such a case, it always has a value smaller than 1, as clearly illustrated in Fig. 4b.

A careful numerical study not presented here revealed that if the exact values of ξ_1 are used, the development of an expression for ξ_2 becomes difficult. This is because in such cases, the value of ξ_2 depends strongly on the end eccentricity besides the slenderness of the column. However, if ξ_1 is limited to unity, the dependence of ξ_2 on end eccentricity is much less so that ξ_2 may be taken as a function of slenderness only. It should be noted that although limiting ξ_1 to unity has the advantage of simplicity, it can make the nominal curvature method un-conservative in predicting the axial load capacity of columns subjected to material failure and with an axial load capacity smaller than N_{bal}. Such a case can happen in a short column with a large end eccentricity. Such a column has a curvature larger than ϕ_{bal}, but its curvature is forced to be ϕ_{bal} in the above approach, which gives rise to the un-conservativeness. Nevertheless, as the slenderness effect in such columns is limited, the un-conservativeness lies within a reasonably small range.

Based on the above discussion, it is suggested that for FRP-confined RC columns, the form of Eq. 17 be retained but N_{bal} be estimated using Eq. 16, leading to:

$$\xi_1 = \frac{N_{bal}}{N_u} = \frac{0.8 f_{cc}^{'} A}{N_u} \le 1 \tag{20}$$

Based on the values of ξ_1 given by Eq. 20, the following equation is proposed for ξ_2 for use in the design of slender FRP-confined circular RC columns:

$$\xi_2 = (1.15 + 0.06\rho_\varepsilon) - (0.01 + 0.012\rho_\varepsilon)\frac{l}{D} \le 1 \tag{21}$$

Eq. 21 was developed though a trial-and-error process for the design equations to provide close predictions to those from the theoretical column model. It should be noted that Eq. 21 ignores the effects of a number of factors, such as the end eccentricity for simplicity in design. It is shown in a later section that Eq. 21 is sufficiently accurate for design use. Eq. 21 reduces to Eq. 19 when no FRP confinement is provided.

4.5 Proposed design equations

With N_{bal}, ξ_1 and ξ_2 determined, the full set of design equations can be given as follows:

$$N_u = \theta\alpha_1 f_{cc}^{'} A\left(1 - \frac{\sin 2\pi\theta}{2\pi\theta}\right) + \left(\theta_c - \theta_t\right) f_y A_s \tag{22a}$$

$$N_u\left(e + \frac{l^2}{\pi^2}\xi_1\xi_2\phi_{bal}\right) = \frac{2}{3}\alpha_1 f_{cc}^{'} AR\frac{\sin^3\pi\theta}{\pi} + f_y A_s R\frac{\sin\pi\theta_c + \sin\pi\theta_t}{\pi} \tag{22b}$$

$$\alpha_1 = 1.17 - 0.2\, f_{cc}^{'} / f_{co}^{'} \tag{22c}$$

$$0 \le \theta_c = 1.25\theta - 0.125 \le 1 \tag{22d}$$

$$0 \le \theta_t = 1.125 - 1.5\theta \le 1 \tag{22e}$$

On the right hand side of Eqs 22a and 22b are the approximate expressions for the section interaction curve. The derivation of this approximate section strength analysis is given in detail elsewhere (Jiang and Teng 2006; Jiang 2008) and only a brief description is given herein. Through the use of an equivalent stress block for FRP-confined concrete and an equivalent steel cylinder for the longitudinal steel reinforcement, these expressions approximate closely the capacity of an FRP-confined RC section as predicted by the conventional section analysis. The definitions of some of the symbols in Eq. 22 are illustrated in Fig. 8. x_n is the depth of the neutral axis (the depth of the equivalent stress block is taken to be $0.9\,x_n$), α_1 is the mean stress factor for FRP-confined concrete, $2\pi\theta$ is the central angle corresponding to the depth of the equivalent stress block, R and A are respectively the radius and the area of the cross section, and A_s is the total area of the longitudinal steel reinforcement. θ_c and

θ_t are variables solely dependent on θ to explain the contributions of compressive and tensile longitudinal steel reinforcements respectively.

When the axial load and the associated initial end eccentricity are known, the design of the FRP jacket should follow the steps listed below:

1) Select the type of FRP and check to see if the slenderness of the column satisfies Eq. 11;
2) Assume a jacket thickness and calculate the compressive strength and the ultimate axial strain of FRP-confined concrete using Eqs 4 and 5;
3) Determine the value of θ through a trial-and-error process until Eqs 22a and 22b are both satisfied;
4) Check to see if the axial load capacity calculated from Eq. 22a is larger than the applied axial load;
5) If step 4) is satisfied, the FRP jacket assumed in step 2) is strong enough to resist the applied axial load; otherwise, increase the jacket thickness and go through steps 2) to 4) again until step 4) is satisfied;
6) If step 4) still cannot be satisfied when the confinement has already been increased to a very high level that exceeds the limit given in Eq. 10, it indicates that the use of FRP in this case is either inefficient or uneconomical, and other means of strengthening should be used instead (e.g. increase the cross-sectional area) or in combination with FRP jacketing.

It should be noted that in the above procedure, it is assumed that all the geometric and material properties of the original RC section are known, as is generally the case in the strengthening of existing RC columns.

Fig. 9 compares a series of interaction curves predicted using the proposed design approach with those produced using the theoretical column model. The interaction curves are for a series of columns of the same section but with a range of slenderness ratios from $\lambda = 10$ to $\lambda = 40$ at an interval of 10. It should be noted that $\lambda = 40$ is slightly larger than the maximum allowable slenderness ratio ($\lambda = 38.75$) defined by Eq. 11. The interaction curves are cut off by a straight line that represents the minimum eccentricity. The parameters used to produce the interaction curves are given in Fig. 9. The approximate curve for $\lambda = 10$ from the design equations is in excellent agreement with the exact curve as the second order effect is very limited at this slenderness value. The approximate curve for $\lambda = 20$ is un-conservative for a certain range of end eccentricities. This overestimation mainly stems from the fact that at this slenderness value, material failure is still the predominant failure mode and this range of end eccentricities corresponds to tensile failure. As a result, the exact nominal curvature found using the simple theoretical model must be larger than ϕ_{bal}, but it is forced to be equal to ϕ_{bal} in the proposed design approach. However, the overestimation is reasonably small and is comparable to that of the current design approach adopted by GB-50010 (2002) for RC columns.

Fig. 10 shows the overall performance of the proposed design approach. The axial load capacities calculated using the simple theoretical model and the proposed design approach are normalized by N_{uo}. Fig. 10 includes the numerical results of all FRP-confined columns of the reduced set of parametric cases listed in Table 2. It can be

seen that the majority of cases fall within the ±10% error lines. The maximum overestimation found among the cases studied is 12.3%.

BS-8110 (1997) specifies that for simplicity, $\xi_1 = 1$ can be used in the design of RC columns with some sacrifice of accuracy; this simplification is always conservative. It should be noted that the simplification of $\xi_1 = 1$ makes the design procedure much more straightforward because otherwise ξ_1 has to be evaluated through a trial-and-error process (ξ_1 is a function of N_u as defined in Eqs 17, 18 and 20). When $\xi_1 = 1$ is adopted in the proposed design approach, the results for the same cases shown in Fig. 10 are as shown in Fig. 11. It can be seen that with this simplification, the predictions become more conservative, but the majority of cases still fall within the ±10% error lines. The maximum underestimation found among the cases studied is 13.5%.

Finally, the proposed design equations were used to predict the axial load capacities of FRP-confined RC columns reported in existing studies (Tao et al. 2004; Fitzwilliam and Bisby 2010; Bisby and Ranger 2010). These column tests have previously been used to verify the rigorous theoretical model (Jiang and Teng 2012a). These columns were all small-scale columns having a diameter of either 150mm or 152mm. The specific properties of these columns are given elsewhere (Jiang and Teng 2012a). The FRP hoop rupture strains used in the design equations when making predictions for the column tests in these three studies are 1.32%, 1.16%, and 1.15% respectively, as found from the corresponding ancillary cylinder tests reported by the original authors. It should be noted that some of the columns do not satisfy the conditions set by Eqs 10 and 11. The columns of Tao et al. (2004) and those cloumns confined with a 2-ply CFRP jacket in Fitzwilliam and Bisby (2010) and Bisby and Ranger (2010) have a $f_{cc}^{'} / f_{co}^{'}$ ratio slightly larger than 1.75. Besides, the columns of Tao et al. (2004) have a slenderness ratio of 33.6 for series C1 and 81.6 for series C2 which exceed the maximum allowable slenderness ratio (30.2) defined by Eq. 11. In the present set of comparisons, series C2 in Tao et al. (2004) was excluded while the remaining columns reported in these three studies were retained. An additional eccentricity was considered when using the design equations to predict the axial load capacities, as required by GB-50010 (2002). GB-50010 (2002) specifies that the additional eccentricity should be taken as the larger of 20 mm and 1/30 of the diameter for circular columns. This provision is for realistically-sized columns; the use of a 20 mm additional eccentricity is thus unreasonable for the small-scale columns under consideration. As a result, an additional eccentricity of $0.05D = 7.5$ mm was used for all the cases under consideration. This value conforms to the minimum eccentricity specified in BS-8110 (1997) (i.e. $0.05D \le 20$ mm). The use of a 7.5mm additional eccentricity was also suggested for modelling Tao et al.'s (2004) column tests in an internal report (Yu et al. 2004) by the same research group that carried out these tests. The axial load capacities predicted using the proposed design equations and the corresponding experimental values are compared in Fig. 12. Fig. 12 shows that the predictions of the proposed design equations are reasonably close to the experimental values and are conservative in most cases.

5 Conclusions

This paper has been concerned with the development of a design method for slender FRP-confined circular RC columns. To this end, a simple theoretical model for slender FRP-confined RC columns was first presented. This model is exclusively for hinged columns with equal end eccentricities (i.e. standard hinged columns) and employs the assumption that the deflected shape of the column is a half-sine wave. Based on the numerical results obtained using the simple theoretical column model, two FRP strengthening limits were then proposed to ensure a safe and economical strengthening design. Finally, a simple design method for slender FRP-confined circular RC columns was formulated based on numerical results from the theoretical column model and following the well-known nominal curvature approach. The simple design equations approximate closely the numerical results obtained using the theoretical column model, and offer safe and close predictions of existing test results for small-scale columns. The results and discussions presented in this paper allow the following conclusions to be drawn:

The effectiveness of FRP confinement decreases as the column becomes more slender, which confirms existing experimental observations. An upper limit for column slenderness was proposed in the paper to ensure an economical strengthening scheme.
While a high level of confinement can greatly enhance the compressive strength of concrete, it may lead to excessive lateral deflections that are not acceptable in practical design. An upper limit for the level of confinement was proposed in the paper to avoid such cases.
A simplified version of the design method with a small sacrifice in accuracy was also presented in the paper. This simplified version is easier for design use and leads to more conservative predictions than the original version.
The test results used to verify the design equations were all obtained using small-scale columns. For further verification of the proposed design method, tests on large-scale slender FRP-confined RC columns need to be conducted in the near future.

Acknowledgements

The authors are grateful for the financial support received from the Research Grants Council of the Hong Kong SAR (Project No: PolyU 5289/08E), The Hong Kong Polytechnic University, and the National Natural Science Foundation of China (Grant No. 51108410). The authors would also like to express their sincere gratitude to Professor Jostein Hellesland at the Mechanics Division of the University of Oslo for his helpful discussions which improved their understanding of the nominal curvature method.

References

Aas-Jakobsen, A. and Aas-Jakobsen, K. (1968). “Buckling of slender columns”, *Bulletin d’ Information, Comite Europeen du Beton*, No. 69, 201-270.

ACI-318 (2008). *Building Code Requirements for Structural Concrete and Commentary*, American Concrete Institute, Farmington Hills, Michigan, USA.

ACI-440.2R (2002). *Guide for the Design and Construction of Externally Bonded FRP Systems for Strengthening Concrete Structures*, American Concrete Institute, Farmington Hills, Michigan, USA.

ACI-440.2R (2008). *Guide for the Design and Construction of Externally Bonded FRP Systems for Strengthening Concrete Structures*, American Concrete Institute, Farmington Hills, Michigan, USA.

Bazant, Z.P., Cedolin, L. and Tabbara, M.R. (1991). "New method of analysis for slender columns", *ACI Structural Journal*, 88(4), 391-401.

Bisby, L.A. and Ranger, M. (2010). "Axial-flexural interaction in circular FRP-confined reinforced concrete columns", *Construction and Building Materials*, 24(9), 1672-1681.

BS 8110 (1997). *Structural Use of Concrete, Part 1. Code of Practice for Design and Construction*, British Standards Institution, London, UK.

Cheng, H.L., Sotelino, E.D. and Chen, W.F. (2002). "Strength estimation for FRP wrapped reinforced concrete columns", *Steel and Composite Structures*, 2(1), 1-20.

CNR-DT200 (2004). *Guide for the Design and Construction of Externally Bonded FRP Systems for Strengthening Existing Structures*, Advisory Committee on Technical Recommendations for Construction, National Research Council, Rome, Italy.

Concrete Society (2004). *Design Guidance for Strengthening Concrete Structures with Fibre Composite Materials*, Second Edition, Concrete Society Technical Report No. 55, Crowthorne, Berkshire, UK.

Cranston, W.B. (1972). *Analysis and Design of Reinforced Concrete Columns*, Research Report 20, Cement and Concrete Association, UK.

De Lorenzis, L., Tamuzs, V., Tepfers, R., Valdmanis, V. and Vilks, U. (2004). "Stability of CFRP-confined columns" Proceedings, *First International Conference on Innovative Materials and Technologies for Construction and Restoration*, 6-9 June, 2004, Lecce, Italy, 327-342.

ENV 1992-1-1 (1992). *Eurocode 2: Design of Concrete Structures – Part 1: General Rules and Rules for Buildings*, European Committee for Standardization, Brussels.

fib (2001). *Externally Bonded FRP Reinforcement for RC Structures*, The International Federation for Structural Concrete, Lausanne, Switzerland.

Fitzwilliam, J. and Bisby, L.A. (2010). "Slenderness effects on circular CFRP-confined reinforced concrete columns", *Journal of Composites for Construction*, ASCE, 14(3), 280-288.

GB-50010 (2002). *Code for Design of Concrete Structures*, China Architecture and Building Press, China.

GB-50608 (2010). *Technical Code for Infrastructure Application of FRP Composites*, China Planning Press, China.

ISIS (2001). *Design Manual No. 4: Strengthening Reinforced Concrete Structures with Externally-Bonded Fibre Reinforced Polymers*, Intelligent Sensing for Innovative Structures, Canada.

Jiang, T. (2008). *FRP-confined RC Columns: Analysis, Behavior and Design*, Ph.D. thesis, The Hong Kong Polytechnic University.

Jiang, T. and Teng, J.G. (2006). "Strengthening of short circular RC columns with FRP jackets: a design proposal", *Proceedings, Third International Conference on FRP Composites in Civil Engineering*, 13-15 December 2006, Miami, Florida, USA, 187-192.

Jiang, T. and Teng, J.G. (2007). "Analysis-oriented models for FRP-confined concrete: A comparative assessment", *Engineering Structures*, 29(11), 2968-2986.

Jiang, T. and Teng, J.G. (2012a). "Theoretical model for slender FRP-confined circular RC columns", *Construction and Building Materials*, 32, 66-76.

Jiang, T. and Teng, J.G. (2012b). "Slenderness limit for short FRP-confined circular RC columns", *Journal of Composites for Construction*, ASCE, doi: 10.1061/(ASCE)CC.1943-5614.0000293.

Kavanagh, T.C. (1960). "Effective length of framed columns", *Proceedings*, ASCE, 86(ST2), 81-101.

Lam, L. and Teng, J.G. (2003). "Design-oriented stress-strain model for FRP-confined concrete", *Construction and Building Materials*,17 (6-7), 471-489.

MacGregor, J.G., Breen, J.E. and Pfrang E.O. (1970). "Design of slender concrete columns", *ACI Journal*, 67(1), 6-28.

Pfrang, E.O. and Siess, C.P. (1961). "Analytical study of the behavior of long restrained reinforced concrete columns subjected to eccentric loads", *Structural Research Series*, No. 214, University of Illinois, Urbana, Illinos, USA.

Tamuzs, V., Valdmanis, V., Gylltoft, K. and Tepfers, R. (2007a). "Behavior of CFRP-confined concrete cylinders with a compressive steel reinforcement", *Mechanics of Composite Materials*, 43(3), 191-202.

Tamuzs, V., Tepfers, R., Zile, E. and Valdmanis, V. (2007b). "Stability of round concrete columns confined by composite wrappings", *Mechanics of Composite Materials*, 43(5), 445-452.

Tamuzs, V., Valdmanis, V., Tepfers, R. and Gylltoft, K. (2008a). "Stability analysis of CFRP-wrapped concrete columns strengthened with external longitudinal CFRP sheets", *Mechanics of Composite Materials*, 44(3), 199-208.

Tamuzs, V., Tepfers, R., Zile, E. And Valdmanis, V. (2008b). "Mechanical behaviour of FRP-confined concrete columns under axial compressive loading", *Fifth International Engineering and Construction Conference (IECC´5)*, 27-29 August, 2008, Irvine, USA, 223-241.

Tao, Z., Teng, J.G., Han, L.H. and Lam, L. (2004). "Experimental behaviour of FRP-confined slender RC columns under eccentric loading", *Proceedings, Second International Conference on Advanced Polymer Composites for Structural Applications in Construction*, University of Surrey, Guildford, UK, 203-212.

Teng, J.G., Chen, J.F., Smith, S.T. and Lam. L. (2002) *FRP-Strengthened RC Structures*, John Wiley and Sons, Inc., UK.

Teng, J.G., Huang, Y.L. Lam. L and Ye L.P. (2007). "Theoretical model for fiber reinforced polymer-confined concrete", *Journal of Composites for Construction*, ASCE, 11(2), 201-210.

Teng, J.G., Jiang, T., Lam, L. and Luo, Y.Z. (2009). "Refinement of a design-oriented stress-strain model for FRP-confined concrete", *Journal of Composites for Construction*, ASCE, 13(4), 269-278.

Yu, Q., Tao, Z., Gao, X., Yang, Y.F., Han, L.H and Zhuang, J.P. (2004). *Research on Seismic Performance of FRP-confined RC Columns with High Axial Load Ratios*, Fuzhou University, China (in Chinese).

Appendix: Notation

A	area of column section
A_s	total area of longitudinal steel reinforcement
e	load eccentricity at column ends
$e_{\min}$	minimum load eccentricity
d	diameter of the circle defined by the centers of the longitudinal steel reinforcement
D	diameter of column section
E_2	slope of second portion of a stress-strain curve for FRP-confined concrete
E_c	elastic modulus of unconfined concrete
E_{frp}	elastic modulus of FRP
E_{seco}	secant modulus at compressive strength of unconfined concrete
E_s	elastic modulus of steel reinforcement
f	lateral deflection of column
f_{mid}	lateral deflection at mid-height of a column
f_{nom}	nominal lateral deflection
f_y	yield strength of longitudinal steel reinforcement
f'_{cc}	compressive strength of FRP-confined concrete
f'_{co}	compressive strength of unconfined concrete
f'_{cu}	cube strength of unconfined concrete
l	length of standard hinged column
M	bending moment
M_{mid}	bending moment at mid-height of a column
M_u	bending moment capacity
M_{uo}	bending moment capacity under pure bending
N	axial load
N_{bal}	axial load at balanced failure

N_u	axial load capacity
N_{uo}	axial load capacity under concentric compression
R	radius of column section
t	thickness of FRP jacket
x	coordinate along column height
x_n	depth of neutral axis
α_1	mean stress factor
ε_c	axial strain of concrete
ε_{co}	axial strain at compressive strength of unconfined concrete
ε_{cu}	ultimate axial strain of FRP-confined concrete
$\varepsilon_{h,rup}$	hoop rupture strain of FRP jacket
ε_t	axial strain at transition point of a stress-strain curve for FRP-confined concrete
ε_y	yield strain of longitudinal steel reinforcement
θ	ratio of central angle corresponding to the depth of the equivalent stress block to 2π
θ_c	factor for contribution of compressive longitudinal steel reinforcement
θ_t	factor for contribution of tensile longitudinal steel reinforcement
λ	slenderness ratio
$\lambda_{\max}$	column slenderness above which FRP confinement has little effect on load-carrying capacity
ϕ	curvature
ϕ_{bal}	curvature at balanced failure
ϕ_{fail}	curvature of critical section at column failure
ϕ_{mid}	curvature at mid-height of column
ϕ_{nom}	nominal curvature
$\phi_{\sec}$	maximum achievable curvature under a given axial load
ρ_K	confinement stiffness ratio

ρ_s	longitudinal steel reinforcement ratio
ρ_ε	strain ratio
σ_c	axial stress of concrete
ξ_1	factor to reflect the effect of axial load level
ξ_2	factor to reflect the effect of column slenderness

Table 1 Entire set of parametric study cases

Parameter	Values
λ	10, 20, 30, 40, 50
e/D	0.05,0.1,0.15,0.2,0.25,0.3,0.4,0.6,0.8
ρ_s	1%, 2%, 3%, 4%, 5%
d/D	0.7, 0.8, 0.9
$f_{cc}^{'}/f_{co}^{'}$	1.25, 1.5, 1.75, 2
ρ_ε	1, 3.75, 7.5

Table 2 Reduced set of parametric study cases

Parameter	Values
λ	10, 20, 30, 40, 50 for $\rho_\varepsilon = 1$
	10, 20, 30, 40 for $\rho_\varepsilon = 3.75$
	10, 20, 30 for $\rho_\varepsilon = 7.5$
e/D	0.05,0.1,0.15,0.2,0.25,0.3,0.4,0.6,0.8
ρ_s	1%, 2%, 3%, 4%, 5%
d/D	0.7, 0.8, 0.9
$f_{cc}^{'}/f_{co}^{'}$	1.25, 1.5, 1.75

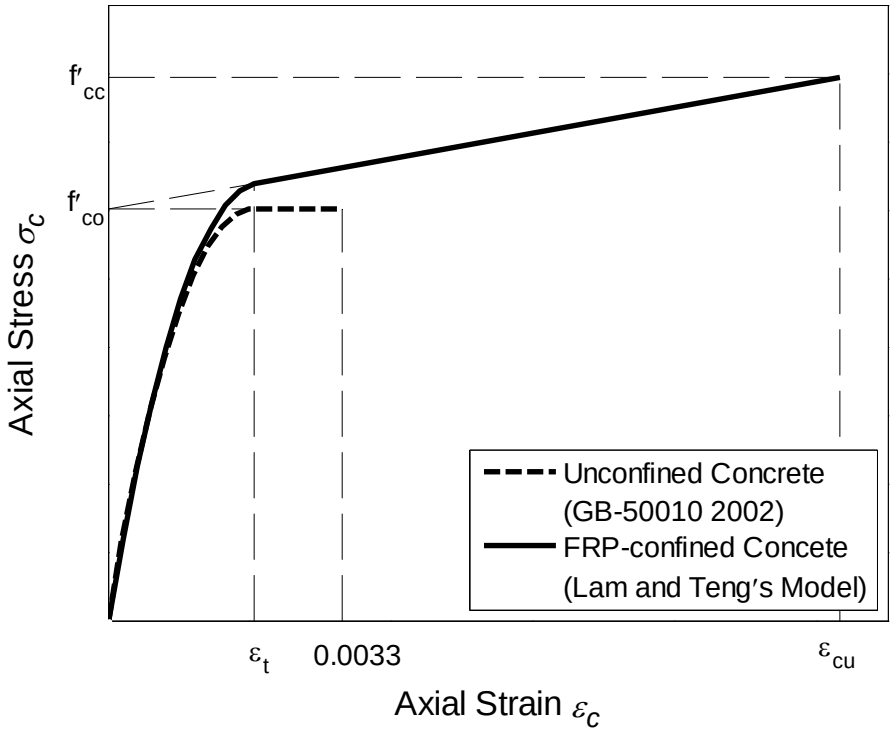

Fig. 1 Lam and Teng's stress-strain model for FRP-confined concrete

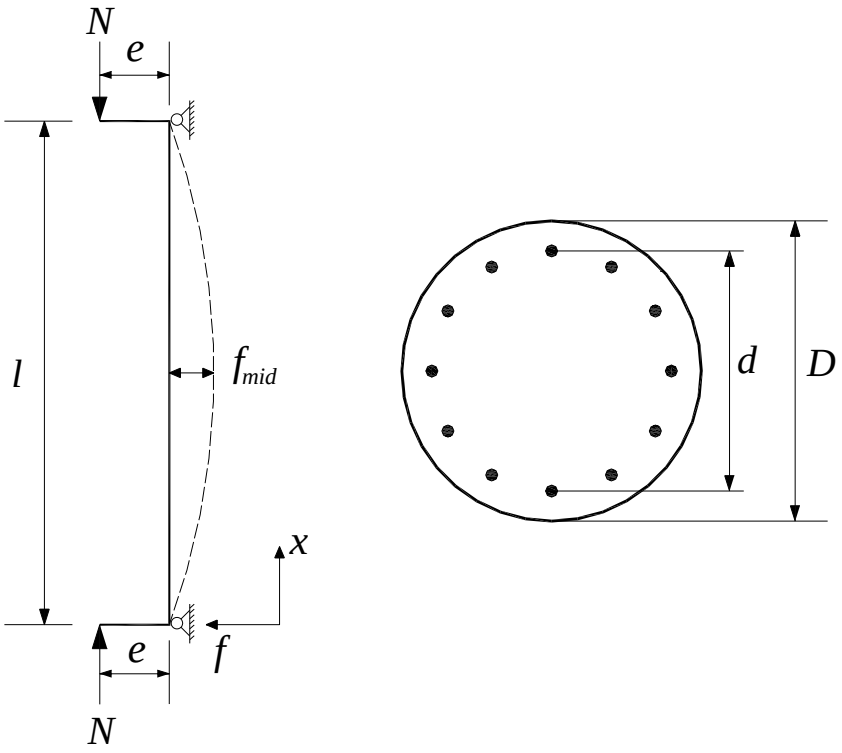

Fig. 2 Standard hinged circular column

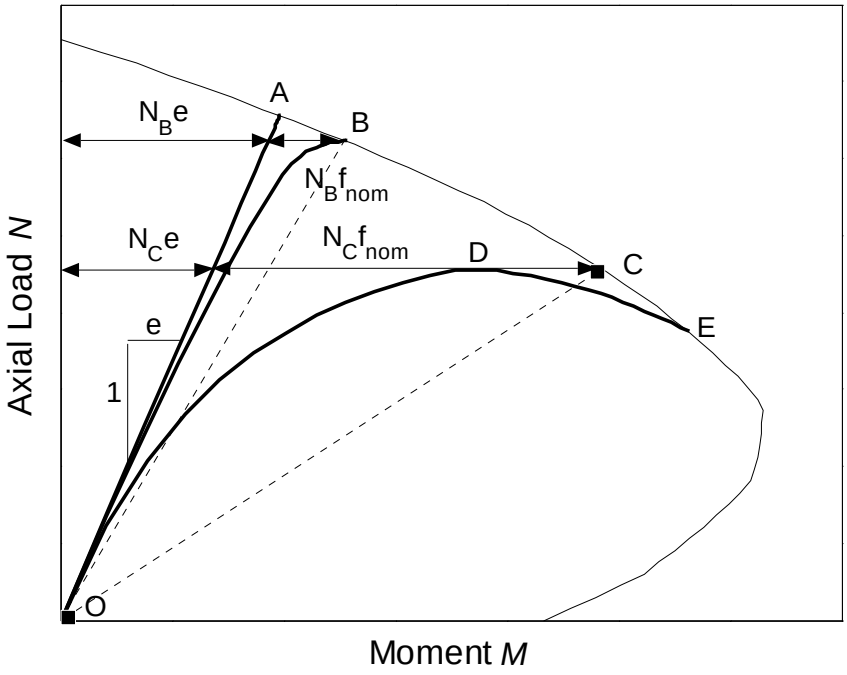

Fig. 3 Definition of nominal lateral displacement

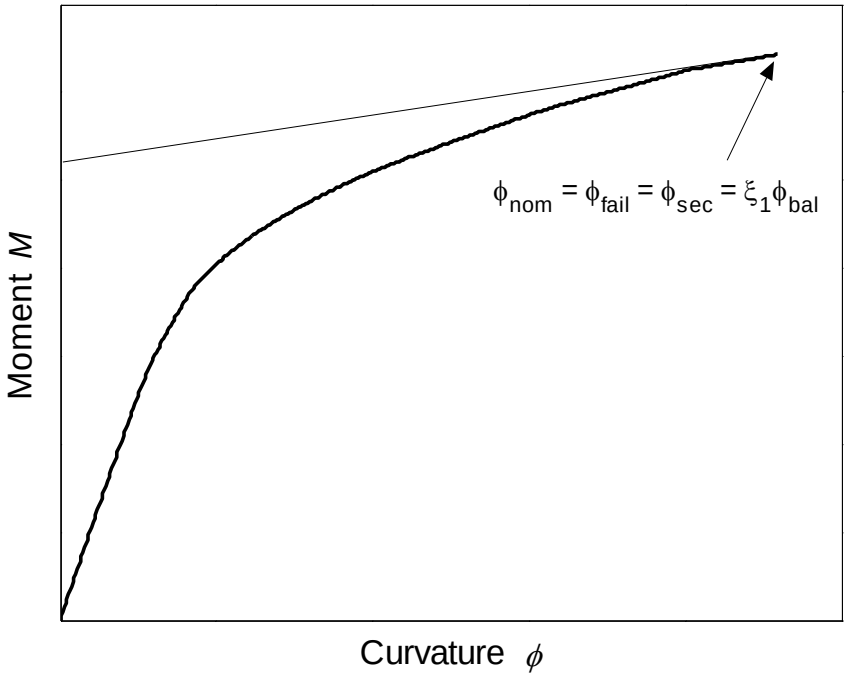

(a) Material failure

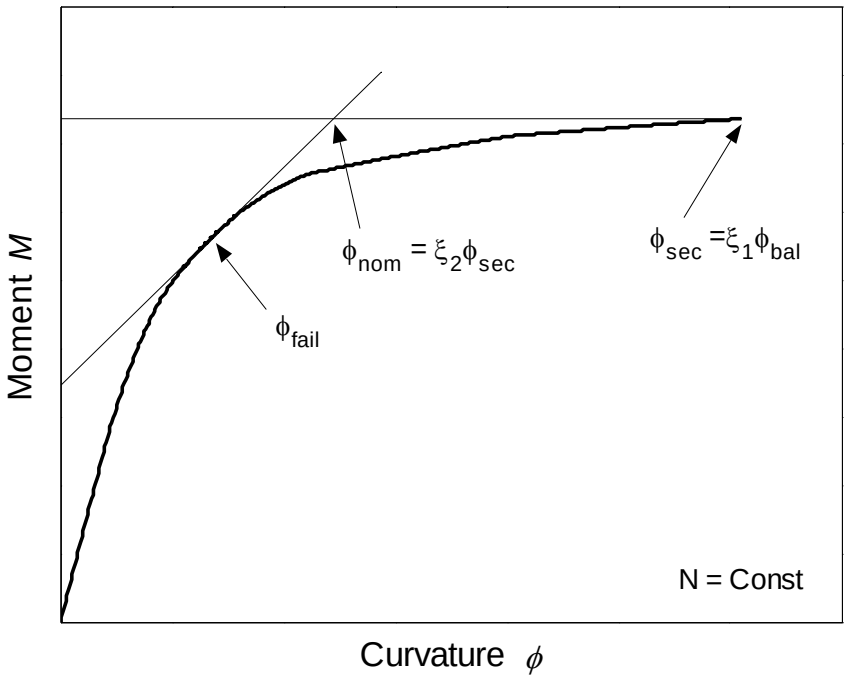

(b) Stability failure

Fig. 4 Determination of the nominal curvature

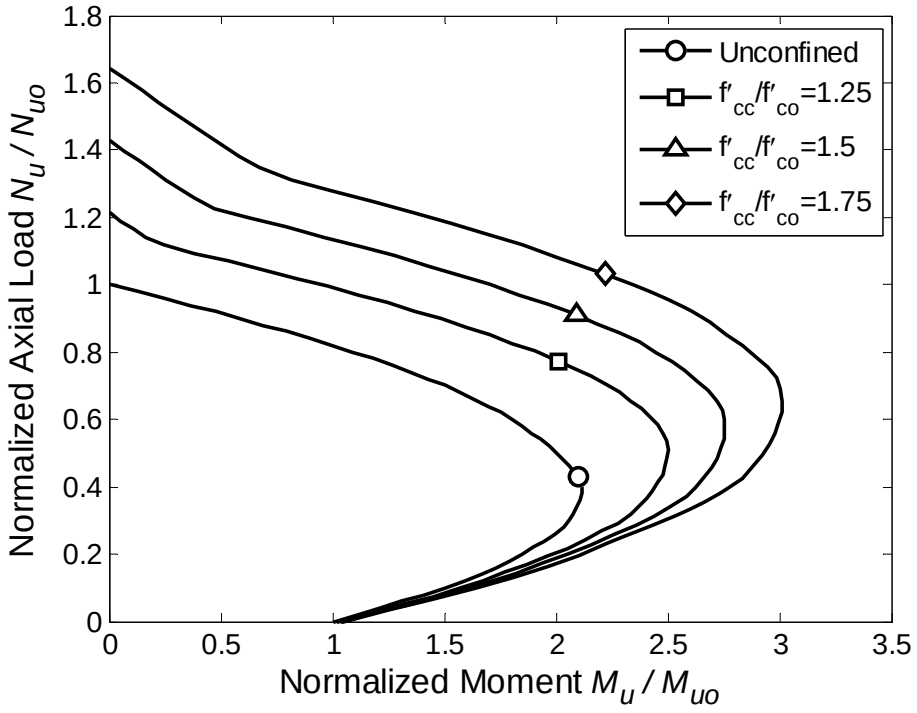

Fig. 5 Axial loads at balanced failure

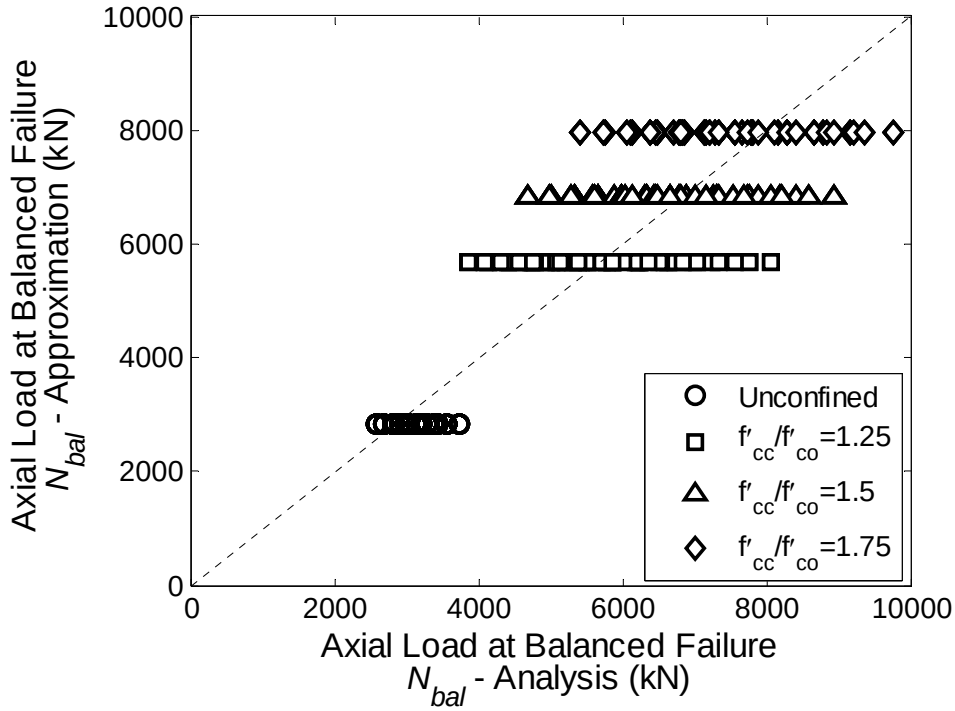

Fig. 6 Performance of Eqs 15 and 16

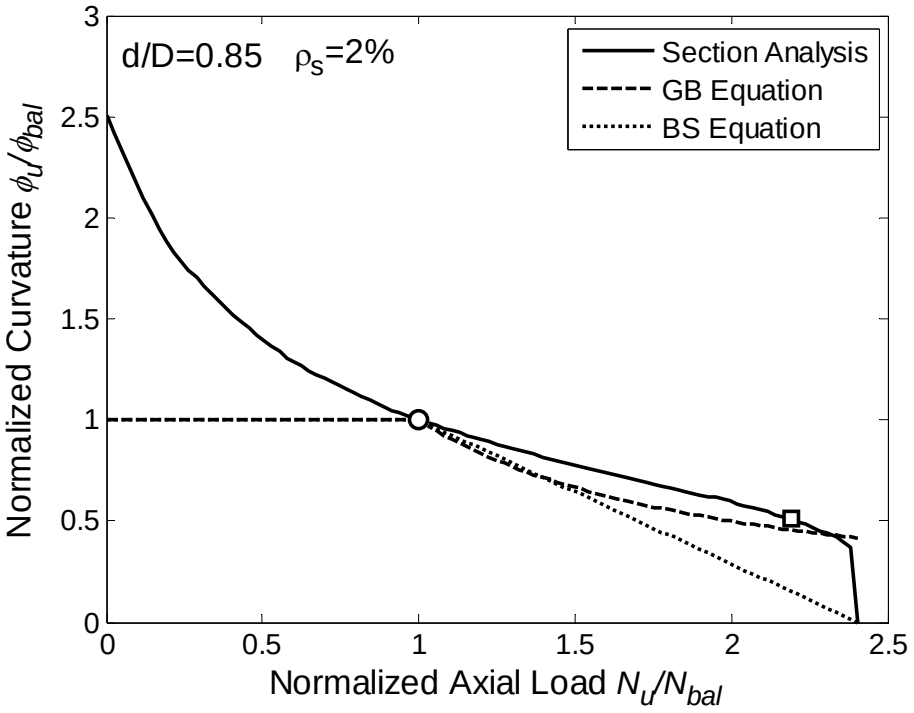

(a) RC section

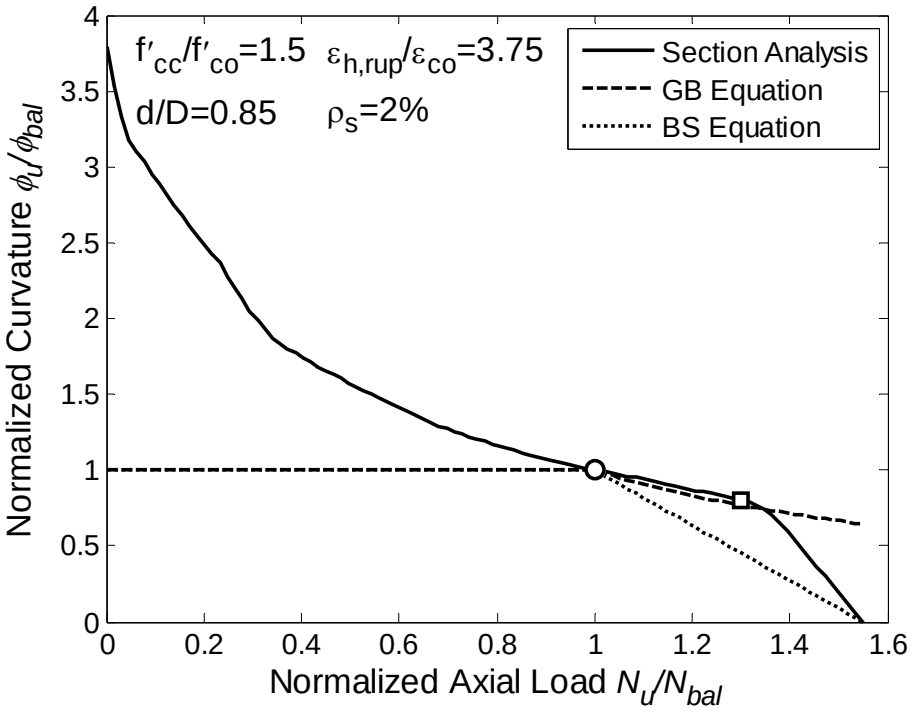

(b) FRP-confined RC section

Fig. 7 Factor ξ_1

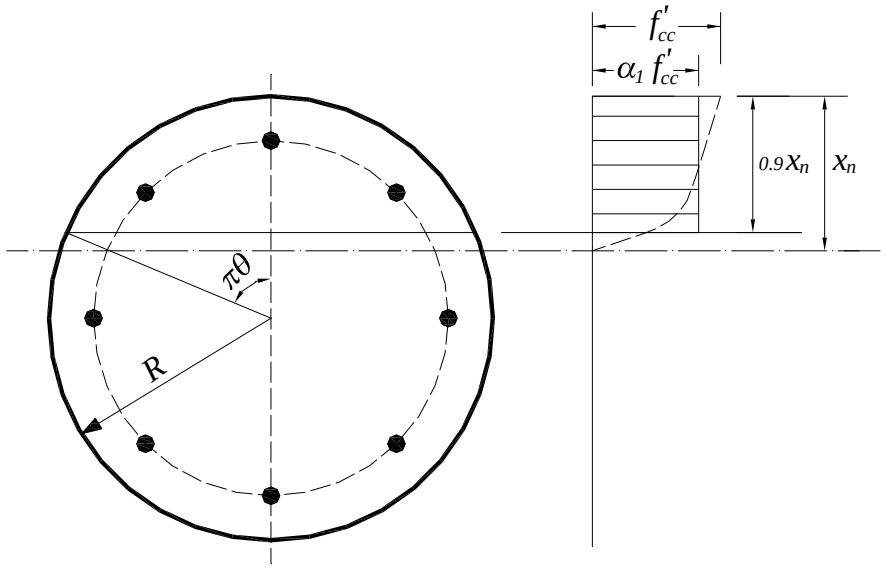

Fig. 8 Equivalent stress block for FRP-confined RC column

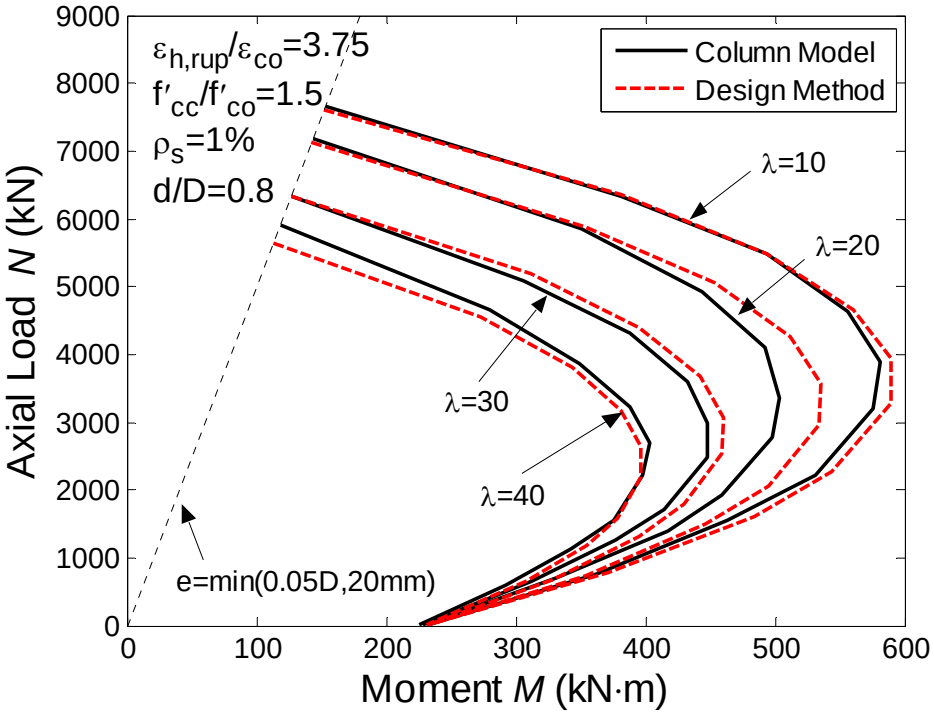

Fig. 9 Typical interaction curves

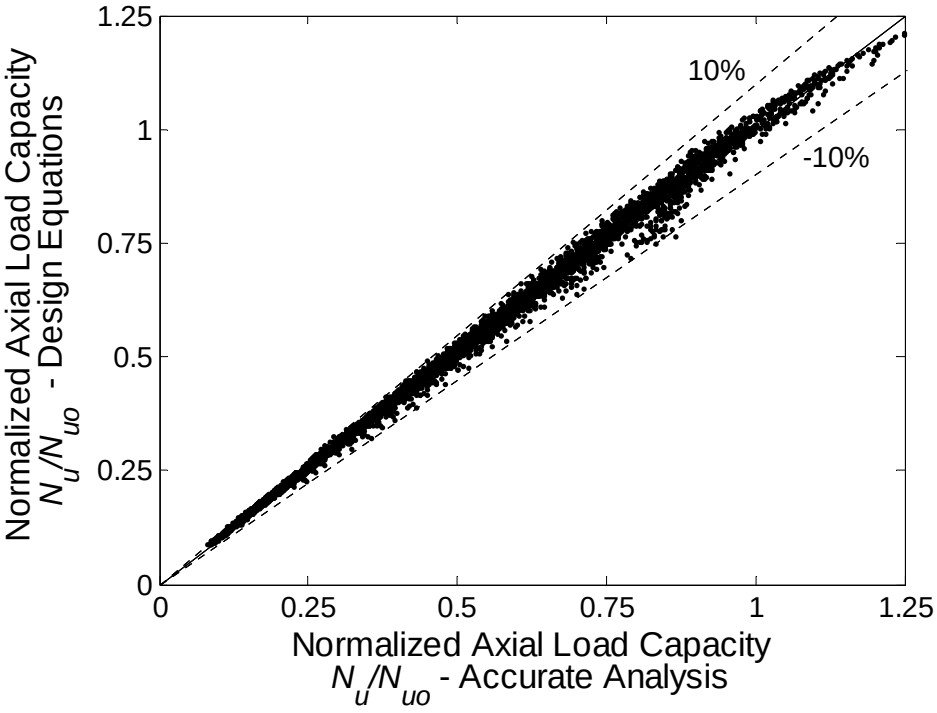

Fig. 10 Performance of the proposed design equations

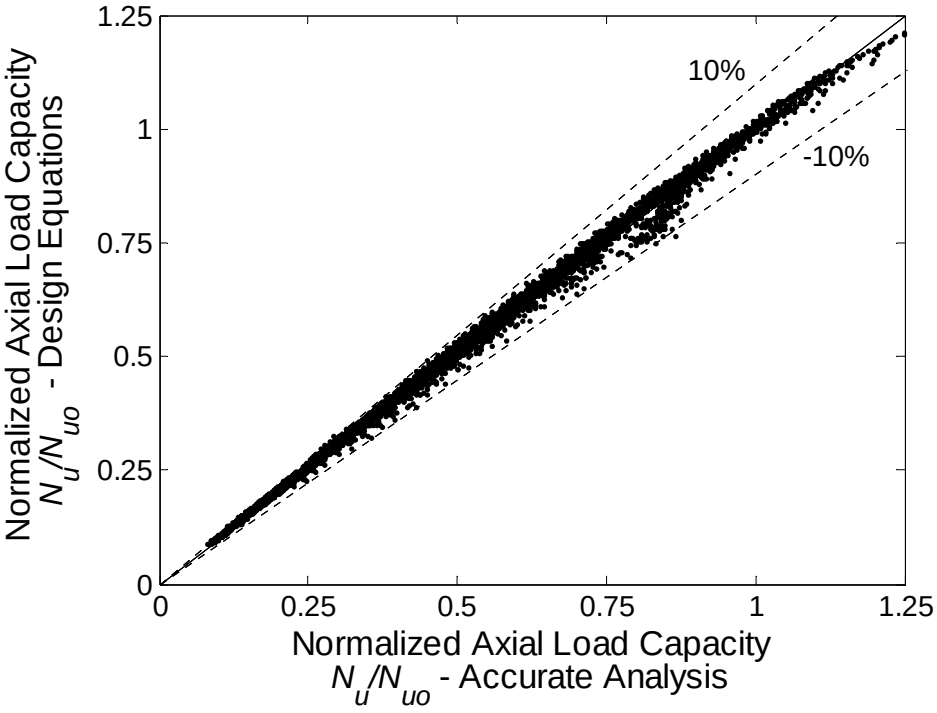

Fig. 11 Performance of the proposed design equations with $\xi_1 = 1$

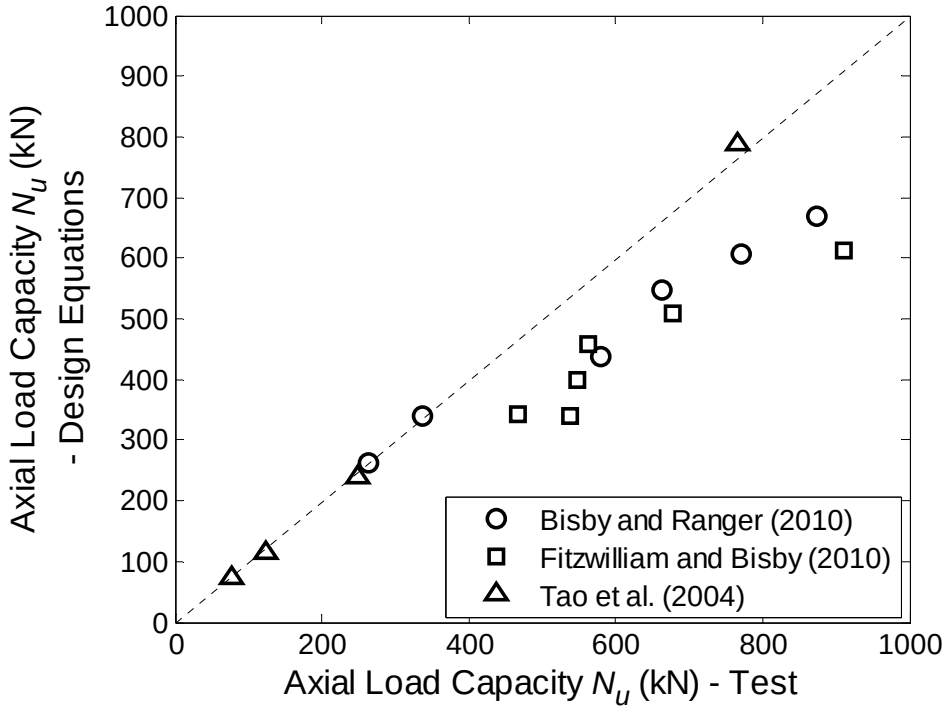

Fig. 12 Predictions of the proposed design equations against test results